Chapter 3

Hardware Specifications

A schematic of the phase modulation device is shown in figure 3.1. The driving current of a laser diode is modulated at a high (radio) frequency, $\omega = 2\pi f$, causing the output of the diode to be intensity modulated. The modulated light passes through the sample medium, and the intensity is monitored using a photomultiplier tube (PMT). A second radio frequency source with an angular frequency of $\omega + \delta\omega = 2\pi(f + \delta f)$ is used to modulate the gain of the detector. 3 mm diameter multimode fiber bundles deliver the modulated light from the laser source to the medium, and from the medium to the PMT.

The current output of the PMT is proportional to the modulated intensity and the modulated gain (as described in more detail below). By modulating the gain, a "mixed" current composed of sum and difference frequencies is generated. The sum and difference frequency signals are passed through a band pass filter centered around the difference frequency, $\delta\omega$. A reference signal is generated in a similar manner by electronically mixing a portion of the two RF signals and then passing the output reference signal through a similar band pass filter centered at $\delta\omega$. The phase and amplitude of the DPDW are measured with respect to the reference signal using traditional lock-in techniques. In our system we typically use a frequency of around $f = 200$ MHz, and an intermediate frequency of $\delta f = 26.6$ KHz.

A great deal of care must be taken when measuring the phase shift. Many electronic devices will measure phase accurately as long as the amplitude of the signal is approximately constant. Since we have an exponentially damped signal, we expect to

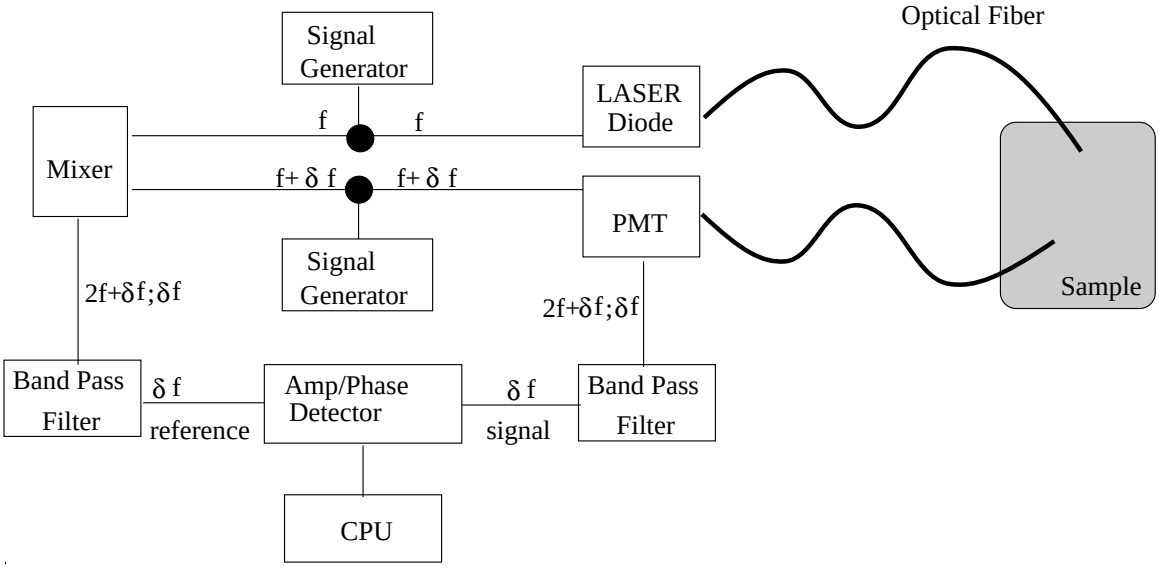

Figure 3.1: A schematic of the frequency domain instrument.

amplitude to vary by more than two orders of magnitude. Each component must be individually tested for amplitude-phase cross-talk. We now discuss each component in more detail.

3.1 Photon Detection - Photomultiplier tubes

For photon detection we typically use a Hamamatsu R928 photomultiplier tube (see specifications in table 3.1). This tube has a spectral sensitivity which extends from 250 nm to 800 nm (see figure 3.2), and a rise time of 2.2 ns. Based on the 2.2 ns rise time, the maximum frequency which can be transmitted is about 72 MHz. In general, as the frequency increases, we see an attenuation of the output of the PMT due to this finite rise time. For this reason we modulate the voltage across the second dynode and pass the lower, intermediate frequency along the dynode chain. Although the choice of which dynode to modulate is somewhat arbitrary, we chose the second dynode so that the input signal is slightly amplified before the modulation. The dc voltage across the second dynode is approximately 100V. To modulate this high voltage we need a 50 Volt sine wave. Using a 50 Ohm source, a 50 Volt modulation

Photocathode material	multialkali
Window material	UV glass
Peak Wavelength	400nm
Anode to Cathode Voltage (max)	1250 V
Average anode current (max)	0.1 mA
Current amplification	1×10^7
Anode dark Current (after 30 Minutes)	2 nA
Rise time	2.2 ns
Transit time	22 ns

Table 3.1: Specifications of the Hamamatsu R928 photomultiplier tube.

requires 1 Ampere of current. To avoid this high current requirement we use a circuit which acts like a transformer to increase the voltage by a factor of 50. To reduce the noise, the circuit is a resonant circuit is designed to pass only the frequency of interest. The specifics of the resonant circuit used for the dynode is beyond the scope of this discussion, and is discussed elsewhere [38].

In a typical PMT configuration, photons strike the photocathode causing electrons to be emitted and subsequently accelerated down the dynode chain [39]. The number of electrons released is proportional to the number of photons striking the photocathode. At each dynode the number of electrons is multiplied, resulting in a total gain of about 10^6. Thus the current output from the PMT is proportional to the incident light intensity ($A\sin(\phi + \omega t)$) and the gain. In our case, both the light intensity and the gain are modulated. So the current output, $i(t)$ is

$$i(t) = K * Light\ Intensity * Gain \tag{3.1}$$

$$= KA\sin(\phi + \omega t) * \sin(\phi_o + \omega t + \delta\omega t) \tag{3.2}$$

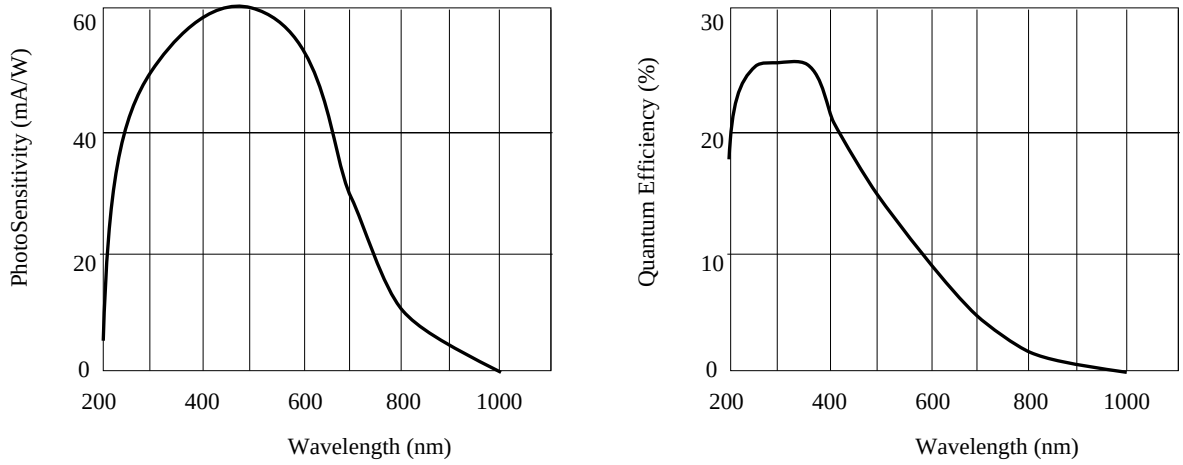

Figure 3.2: The spectral sensitivity and quantum efficiency of the R928 PMT.

$$= (KA/2)\left[\delta\omega t) + \cos(\phi - \phi_o - \delta\omega t) + \cos(\phi + \phi_o + 2\omega t\right] \tag{3.3}$$

K and ϕ_o are constants which depend on the gain, losses, lengths of cables, etc.[40]. They are both independent of the sample being measured. Here we have used the identity

$$sin(A) * sin(B) = \frac{1}{2}\left\{cos(A-B) - cos(A+B)\right\}. \tag{3.4}$$

This output is passed through a band pass filter and the phase, ϕ, is measured at the intermediate frequency, $\delta\omega$ using traditional lock-in techniques.

$$Measurement = \frac{AK}{2}\left[\sin(\phi + \phi_o + 2\omega t + \delta\omega t) + \sin(\phi - \phi_o - \delta\omega t)\right] \tag{3.5}$$

$$\stackrel{filter}{\rightarrow} \frac{AK}{2}\sin(\phi - \phi_o - \delta\omega t) \tag{3.6}$$

In a typical experiment we use a medium with a reduced scattering coefficient of 6-10 cm^{-1} and an absorption of 0.02 cm^{-1}. In this medium, a detector 6 cm from the source with a collection area of 0.1 cm^2, and an efficiency of 1%, we will detect about 10^8 photons/second. Using a 3 mW laser diode at 800 nm, this corresponds to 3 pW. With a photosensitivity of 20 mA/W and a gain of 10^6, the output current is about 60×10^{-9}A. We use a load resistor of 10kΩ, so the output voltage from the

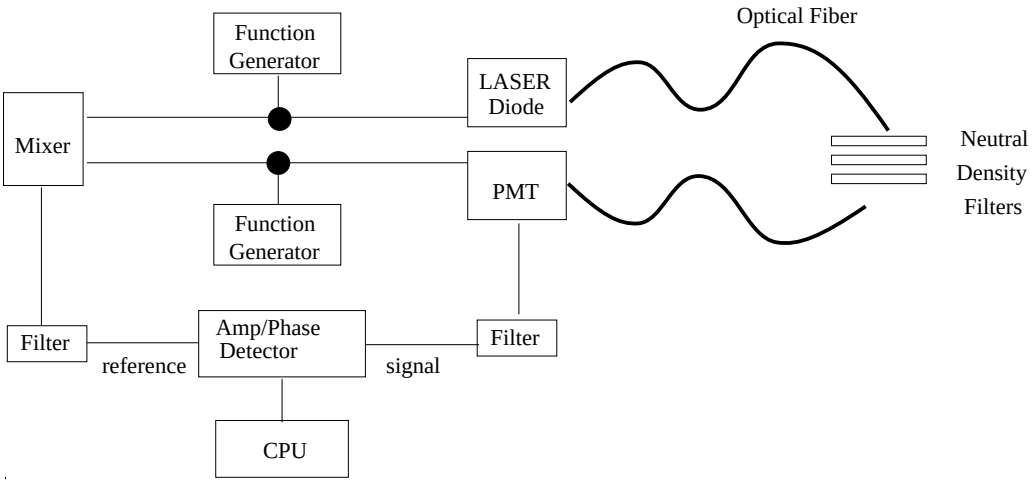

Figure 3.3: Experimental setup for testing the amplitude-phase cross-talk of the PMT.

photon detection system is 0.6 mV. The band-pass filter has a gain of about 100, so the input to the lock-in is on average 60 mV.

Most electronic circuits suffer from the characteristic that the phase of the wave shifts if the amplitude changes (amplitude-phase cross-talk). To test the amplitude-phase cross-talk of the PMT, neutral density filters are placed between the source and detector to change the amplitude and phase in a manner similar to experiment (see figure 3.3). We have experimented with different types of PMT's, with and without gain modulation, and in all of these systems, there is serious amplitude-phase cross-talk in the PMT. Later experiments showed that there are at least two effects contributing to the amplitude-phase cross-talk.

In the course of investigating the amplitude-phase cross-talk in the PMT, we discovered that the phase measurement changes considerably depending on where the photons hit the photocathode. The dynode structure of the R928 is shown in figure 3.4, left panel. The distance which the photoelectrons travel from the photocathode to the first dynode varies a few millimeters depending on where the the photon strikes the photocathode. The photoelectrons are in a 100V potential and therefore travel at a speed of about 2×10^7 m/s. With a 200MHz signal, this gives a photoelectron wave a wavelength of about 2 cm. A 2 mm change in pathlength then corresponds

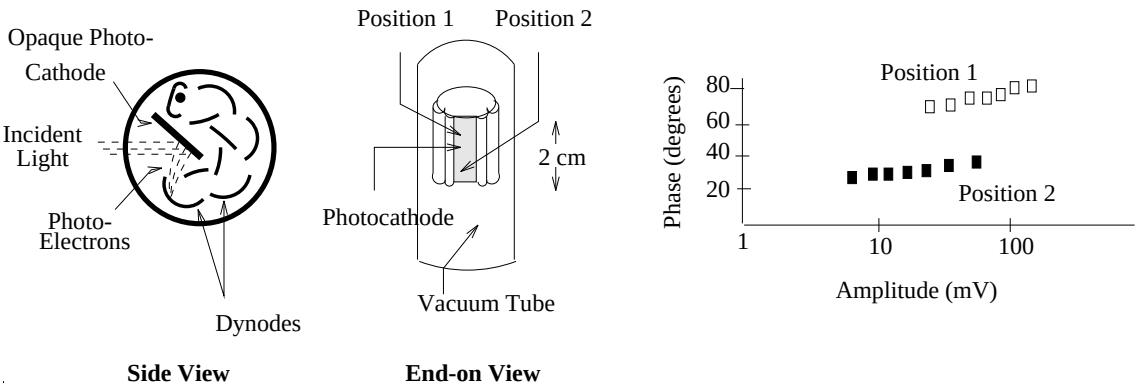

Figure 3.4: The dynode structure and position sensitivity of the R928 PMT.

to a 36° change in phase. This phase shift is evident in figure 3.4 (right panel) where the amplitude-phase cross-talk has been observed when the optical fiber is placed near two different locations on the photocathode. We can minimize this effect by focusing the light from our fiber bundle onto the PMT. We found that focusing the light slightly reduces the noise, but does not eliminate the amplitude-phase cross-talk in the PMT.

We also discovered that we were encountering an effect called space-charge coupling. (Basically, as the charge passes down the dynode chain, each electron adds to the effective electric field. This effects the total electric field that each electron feels.) To demonstrate this effect, we did the following experiment. Again, the source and detector were separated by neutral density filters. A small tungsten lamp was attached near the source. As we changed the current driving the lamp, we detected an increase in the DC current from the PMT, and a change in phase of the AC signal (see figure 3.5). In a perfect system, without the problem of a space-charge coupling, the DC light would not have affected the phase. Next we investigated two methods to stabilize the dynode currents. First we tried to use the lamp to stabilize the DC signal from the PMT. As we added neutral density filters, we monitored the DC output from the PMT, and altered the lamp current to stabilize this DC output. This feedback mechanism decreased the amplitude-phase cross talk. (See figure 3.5).

We also investigated stabilizing the dynode voltages by inserting 150V Zener

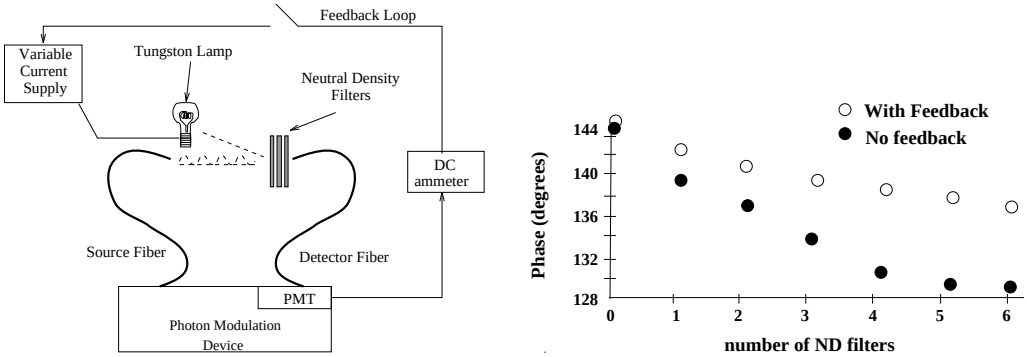

Figure 3.5: Holding the DC current from the PMT constant reduces the amplitude-phase cross-talk.

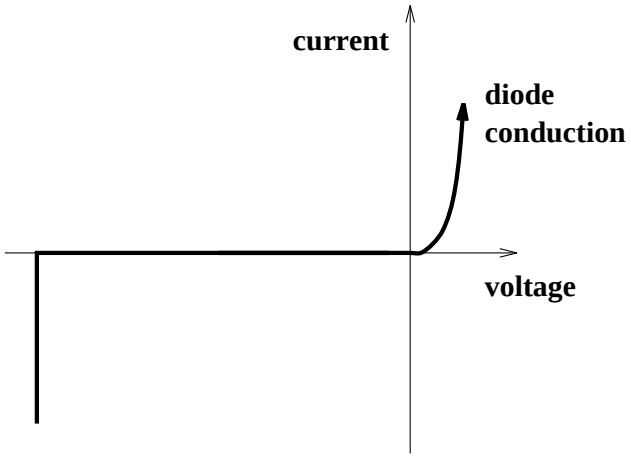

Figure 3.6: The current versus voltage curve of an ideal zener diode.

diodes into the dynode chain (see figure 3.7). Zener diodes have a dynamic resistance and are used to create a constant voltage in a circuit (see figure 3.6). This also decreased the amplitude-phase cross-talk. But neither the DC feedback nor the Zener diode solution were adopted in practice. Instead, we changed detectors from a PMT to an avalanche photodiode (APD).

3.2 Photon Detection - Avalanche Photodiodes

The following discussion of avalanche photodiodes was adapted from the Hamamatsu Photodiode catalog [41].

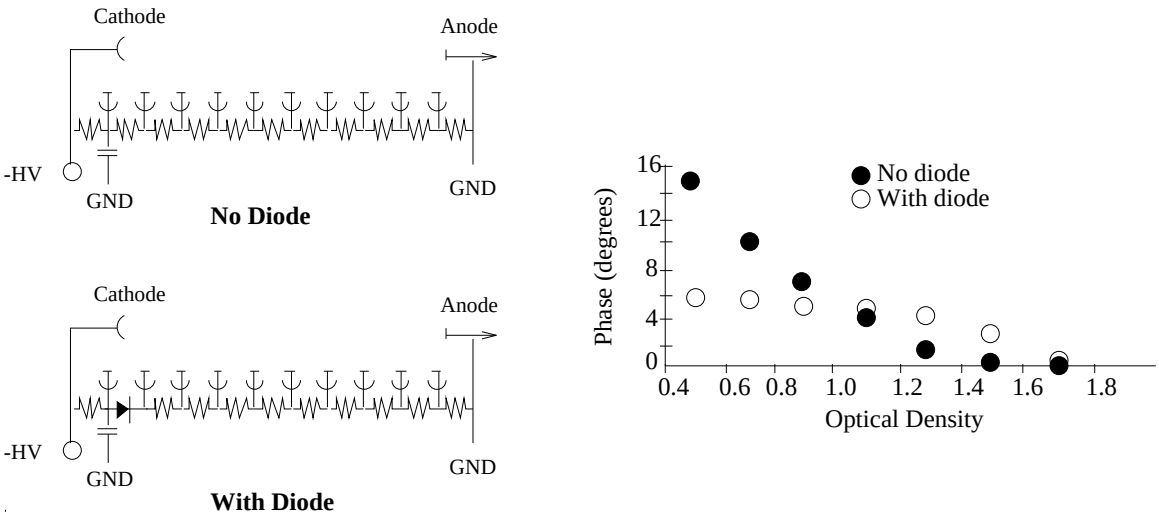

Figure 3.7: A Zener diode is used to reduce the space-charge effect on the phase.

Photodiodes are semiconductor light sensors that generate a current or voltage when the P-N junction of the semiconductor is illuminated by light. Figure 3.8 shows a cross section of an avalanche photodiode. The P-layer material at the active surface and the N material at the substrate form a P-N junction which operates as a photoelectric converter. The usual P-layer for a silicon photodiode is formed by selective diffusion of boron, to a thickness of approximately 1μm or less and the neutral region at the junction between P- and N- layers is known as the depletion layer. By varying and controlling the thickness of the various layers and doping concentrations, the spectral response and frequency range can be controlled.

When light strikes a photodiode, electrons within the crystal structure become stimulated. If the photon energy is greater than the band gap, the electrons are pulled up into the conduction band, leaving holes in their place in the valence band. This results in a positive charge in the P-layer and a negative charge in the N-layer. In an external circuit is connected between the P- and N-layers, electrons will flow away from the N-layer, and holes will flow away from the P-layer towards the opposite respective electrodes.

When a reverse voltage is applied to a PN junction, electrons generated by the

Active area	0.19 mm^2
Window material	borosilicate glass
Peak Wavelength	800nm
Anode to Cathode Voltage (max)	200 V
Current amplification (without external amplifier)	1×10^2
Dark current	0.1 nA
Frequency range (equivalent to rise time)	1MHz - 1GHz

Table 3.2: Specifications of the Hamamatsu C5658 Avalanche photodiode.

incident light collide with atoms in the field and produce secondary electrons. This process occurs repeatedly. This is known as the avalanche effect, and since it results in the signal being amplified, this type of device is ideally suited for detection of low light levels.

The APD we used was a Hamamatsu C5658, and the specifications are given in table 3.2. This particular APD has a built-in bias supply, current to voltage converter and a low noise, broad band amplifier.

Because the APD is compact, there are virtually no path length variations as in the photomultiplier tube. We were not able to detect any amplitude-phase cross-talk using the APD, although Yokoyama *et al.* [42] have detected a small amplitude-phase cross-talk in the APD at 1 GHz. In addition, the sensitivity range of the APD extends much further into the infra-red (400 nm - 1000 nm for the APD, (figure 3.9,) 400 nm - 800 nm for the PMT). The disadvantages of the APD are its small active area (0.5 mm) and low gain (with a built in low noise amplifier the ADP module gain is 10^5 compared to the PMT gain of 10^6). Finally, the response of the APD is fast enough

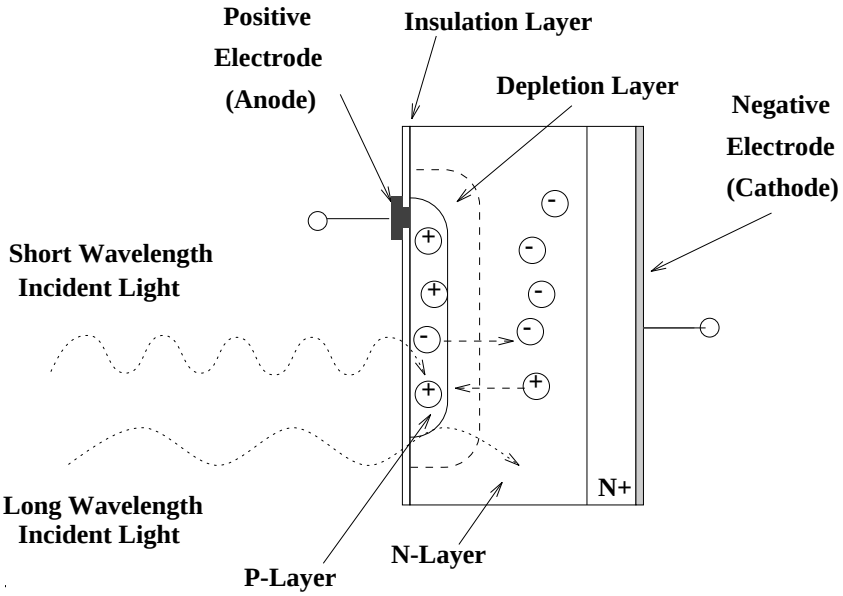

Figure 3.8: Schematic of a silicon photo-diode.

that we do not need to modulate the gain, instead we mix the output with the second frequency in an external mixer.

3.3 Laser diodes

The laser diodes we employed are standard 5 mW diodes, mainly used in laser printers and bar code readers (Sharp LT022DC). We modulate the DC driving current to oscillate between the lasing threshold and the maximum current using a standard capacitor coupling (see figure 3.10). The DC driving circuit is a standard chip which may be purchased from Sharp (Sharp IR3C01). A home-made driving circuit is described elsewhere [38]. We have also investigated using light emitting diodes (LED's) as light sources, but LED's are difficult to modulate at high (above 20 MHZ) frequencies.

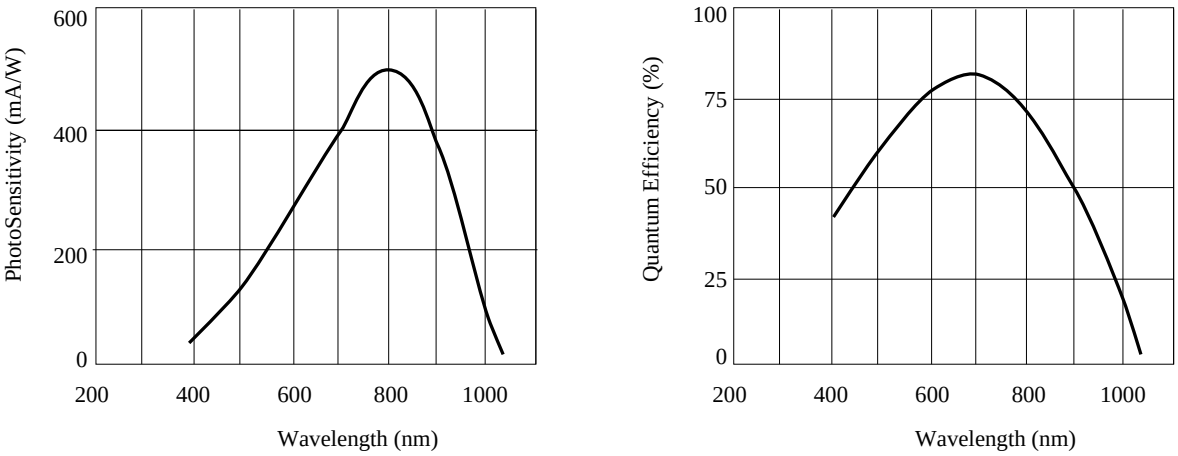

Figure 3.9: The spectral sensitivity and quantum efficiency of the photodiode in an APD. Note that because the APD has an internal gain (x100), the sensitivity and efficiency should be multiplied by a factor of 100.

High speed response	greater than 1 GHz
Optical Power Output	5 mW
Operating Temperature	-10 to +60° C
Threshold Current	50 mA
Operating Current	65 mA
Operating Voltage	0.9 V
Wavelength	780 nm

Table 3.3: Specifications of the Sharp LT022MD laser diode.

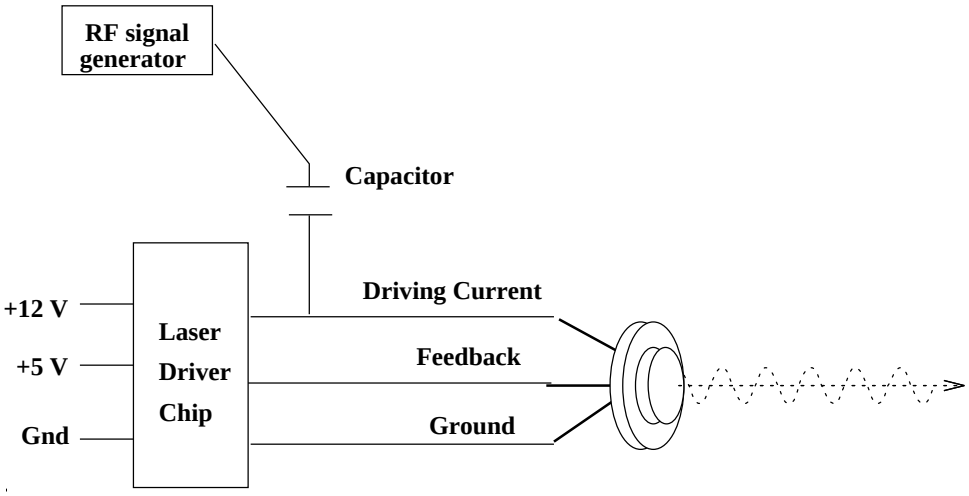

Figure 3.10: An AC signal is capacitor coupled to the laser diode driving current.

3.4 Amplitude-phase detector

In our studies we have employed a Stanford Research Systems (SRS530) Lock-In Amplifier for our phase detector. The SRS530 is a dual phase detector, which means that it detects both amplitude and phase. A schematic of the lock-in amplifier is shown in figure 3.11. A signal, $A\sin(\omega t+\phi)$, and a reference wave, $\sin(\omega t)$, are input and the reference is split internally into two channels. One channel is shifted by 90° . Each of these channels multiplies the signal, and the products are sent through band pass filters,

$$X = A\sin(\omega t+\phi) * \sin(\omega t) \tag{3.7}$$

$$= \frac{A}{2}\left\{-\cos(2\omega t+\phi)+\cos(\phi)\right\} \tag{3.8}$$

$$\overset{band\ pass\ filter}{\rightarrow} \frac{A}{2}\cos(\phi) \tag{3.9}$$

$$Y = A\sin(\omega t+\phi) * \cos(\omega t) \tag{3.10}$$

$$= \frac{A}{2}\left(\sin(2\omega t+\phi)+\sin(\phi)\right) \tag{3.11}$$

$$\overset{band\ pass\ filter}{\rightarrow} \frac{A}{2}\sin(\phi) \tag{3.12}$$

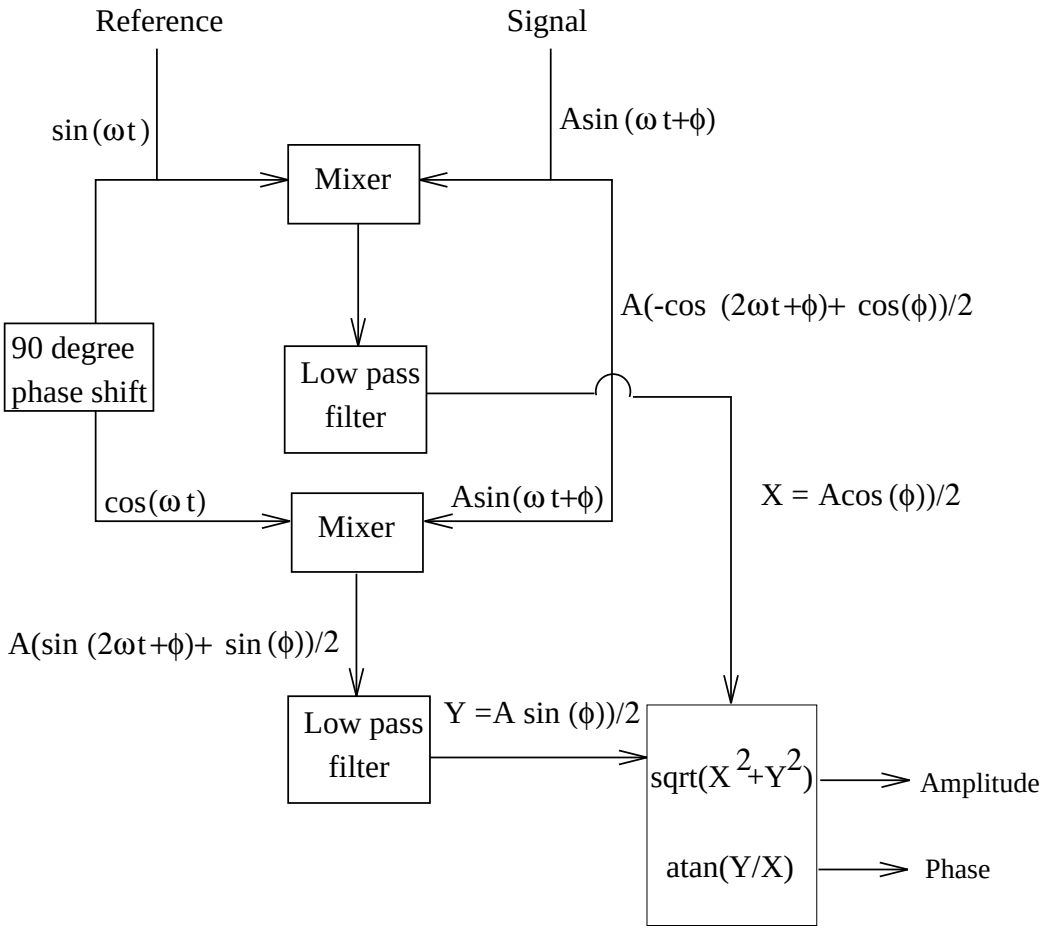

Figure 3.11: A schematic of the lock-in amplifier.

Here we have used the identities

$$sin(A) * sin(B) = \frac{1}{2}\left\{cos(A-B) - cos(A+B)\right\} \tag{3.13}$$

$$sin(A) * cos(B) = \frac{1}{2}\left\{sin(A-B) + sin(A+B)\right\}. \tag{3.14}$$

The lock-in will provide either these XY components, or internal circuitry will return the amplitude and phase,

$$amplitude = \sqrt{X^2 + Y^2} \tag{3.15}$$

$$phase = \tan^{-1}(Y/X) \tag{3.16}$$

Sensitivity	100 nV to 500 mV
Signal Filters	60 Hz notch 120 Hz notch bandpass (Q = 5)
Frequency	0.5 Hz to 100 kHz

Table 3.4: Specifications of the SRS530

A GPIB or RS232 interface allows direct data input from, and control of the SRS530. Some additional specifications are shown in table 3.4.

To make sure that the SRS530 records the phase and amplitude correctly over a wide range of amplitudes, we split the output from a standard low frequency function generator as shown in figure 3.12. One side is used as the reference signal, and the other is passed through a variable attenuator (Kay brand, model 839) before being input into the measurement channel. The results shown in figure 3.12 show the lock-in is capable of measuring the phase to within 0.2° when the amplitude changes from 1 mV to 500 mV.

3.5 Signal Generators

There are a variety of choices for the signal generators. In our lab, we used either home-made resonant circuits designed from crystal oscillators [38] or 220 MHz radio transceivers (Kenwood TM-321A) which happened to be in the lab. The phase stability of the radio transceivers (about 0.2 KHz/hour frequency drift) is much better than the home-made generators (about 2 kHz/hour frequency drift). But the frequency of each radio transceiver is still apt to drift, especially with changes in temperature. Although this drift is small compared to the RF frequency, it is critical when we try to measure at an intermediate frequency. For example, a 0.002% frequency shift of

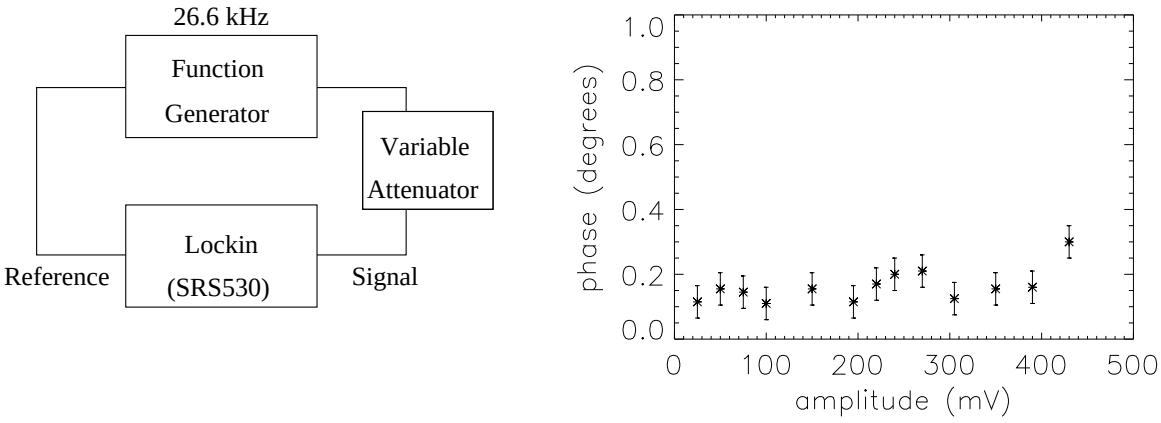

Figure 3.12: Amplitude-phase cross-talk of the SRS530. The error in the SRS530 phase measurement in this configuration is +/- 0.1° .

one of the signal generators at 200 MHz results in a 4 kHz shift in the intermediate frequency. Since our band pass filters are set at a particular frequency with a full width half max of about 5 kHz, a 4 kHz drift is unacceptable. Recently, we have purchased variable signal generators (9 kHz - 2 GHz, Rhode & Schwartz SMY02). These signal generators use a few lower frequency crystal oscillators, and the frequencies are multiplied and combined appropriately to create the desired frequency. These generators have a major advantage over the radio transceivers in that two generators can be phase locked, that is, the crystal from one generator can be used to drive the second generator. On the Rhode & Schwartz, this is done using a single cable to connect the 10 MHz reference on one signal generator to the 10 MHz reference on the other and turning on the 'external reference' switch. Using the same crystal to drive both generators ensures the stability of $\delta\omega$ (less than 0.1 kHz/hour drift [43]). The only disadvantage to the Rhode & Schwartz is the cost (about $7,000) and the physical size of the device.

3.6 Filters

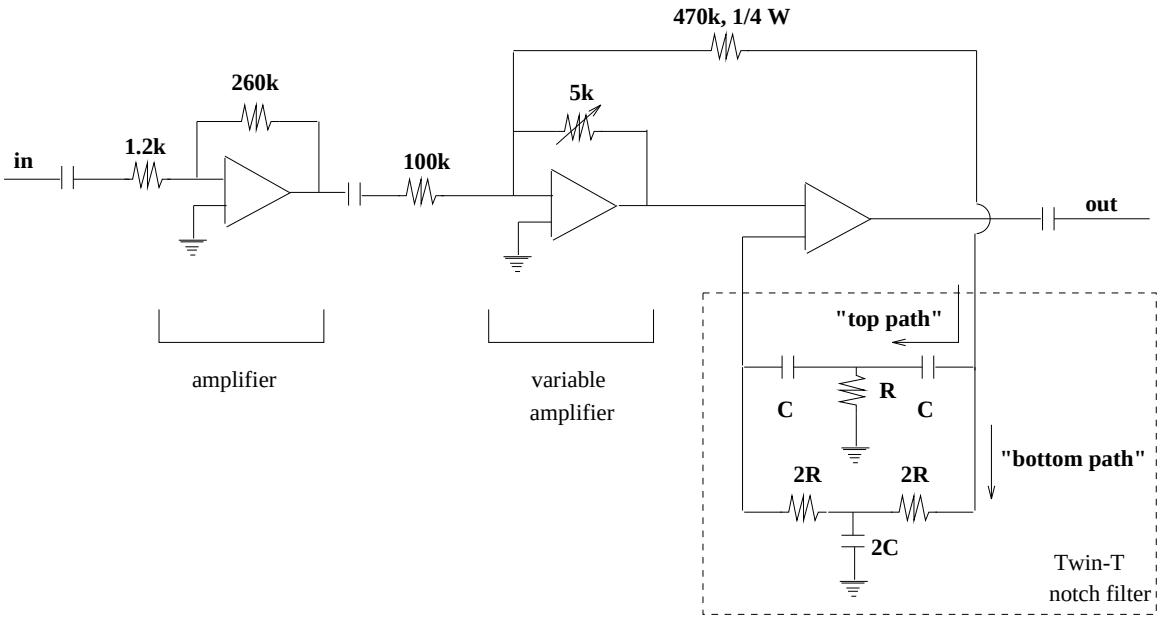

Figure 3.13: The twin-T active bandpass filter.

Our initial experiments used the twin-T band bass filter shown in figure 3.13. In the twin-T band-pass filter, the signal is first amplified, and then split. One part of the signal passes through a second, variable amplifier, and the second part passes through the twin-T *notch* filter. The two signals are then recombined in a differential amplifier. In this way, we have used the sharp attenuation properties of the twin-T *notch* filter to create a sharp *spike* filter. The Q of a filter is defined as the central frequency divided by the full width at half max. In this filter the Q is adjustable, by changing the variable 5k resistor in the second amplifier. The capacitors are to eliminate any DC signal. The performance of this filter is demonstrated for several Q in figure 3.14. Typically we use a Q of about 5.

The twin-T notch filter works by combining two signals that are 180° out of phase. The top path is a high pass filter with a characteristic frequency $\omega_c = 1/RC$, and the bottom path is a low pass filter with the same characteristic frequency. Because the top path has passed through two capacitors, the phase is shifted 180° . Thus at ω_c the two signals interfere destructively giving a deep amplitude null. Theoretically,

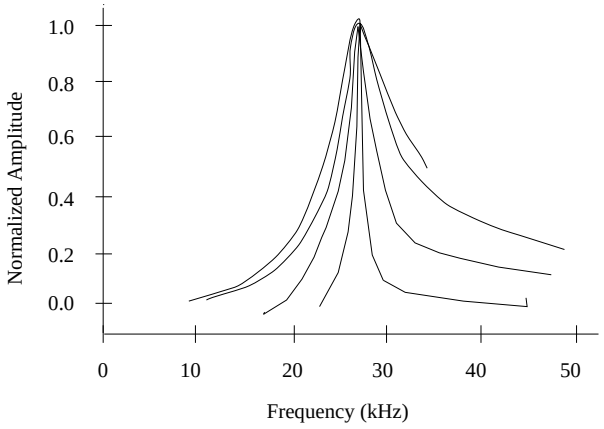

Figure 3.14: The response of the twin-T band-pass filter at several different Q.

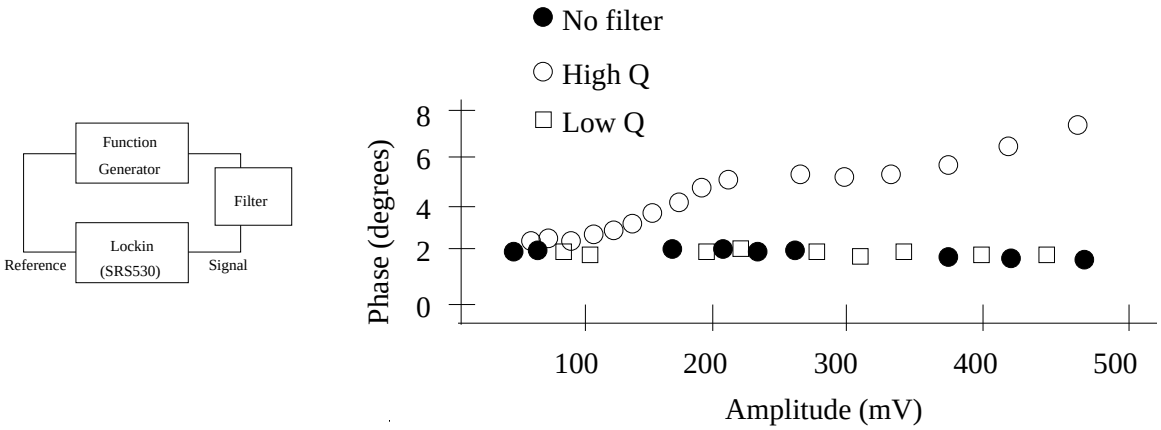

Figure 3.15: Amplitude-phase cross-talk of the twin-T filter. All traces have been shifted to 0° for comparison purposes.

the twin-T has infinite attenuation at ω_c.

When we tested the amplitude-phase cross-talk of the twin-T, it did not perform well (see figure 3.15). Basically, as we decreased Q, the amplitude-phase cross-talk was less critical, but the noise was too large.

Next we tried the passive filter shown in figure 3.16. This filter is actually two separate RLC filters, (center frequency, $\omega^2 = 1/LC$) isolated from each other by a small capacitor. This capacitor also acts to further reduce the DC signal. The Q of this filter is about 5. Figure 3.17 demonstrates that the amplitude-phase cross-talk is negligible.

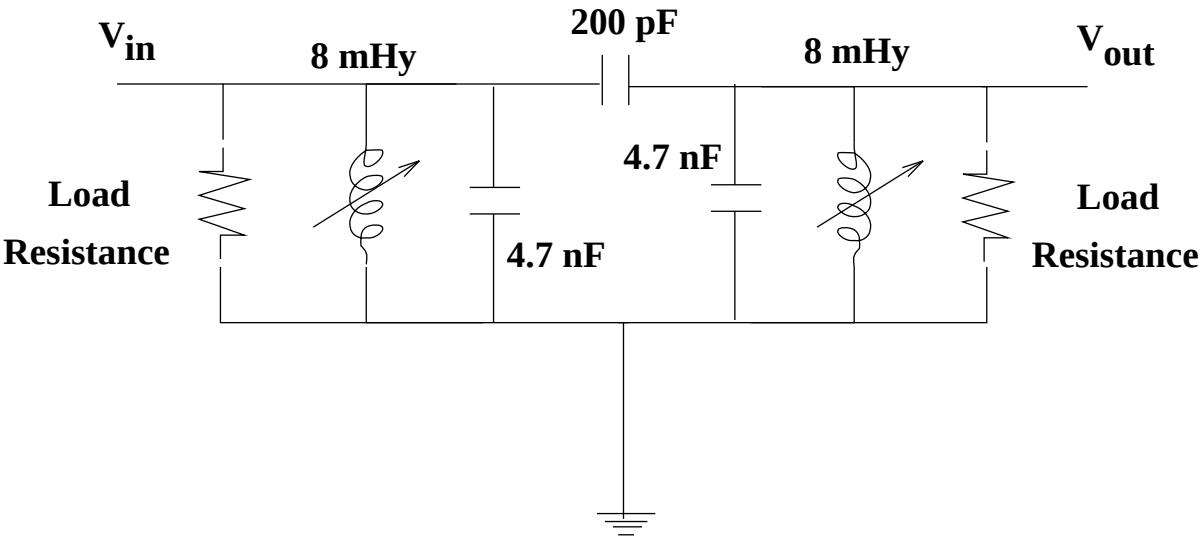

Figure 3.16: A passive bandpass filter. Designed and constructed by Ken Simmons, Philadelphia, Pennsylvania.

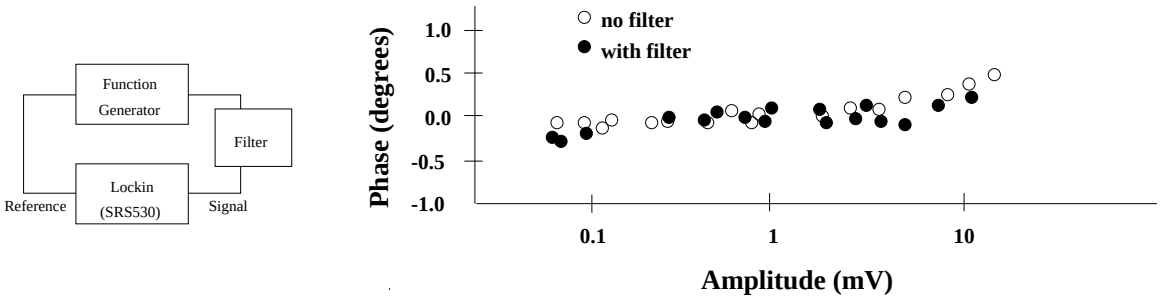

Figure 3.17: Amplitude-phase cross-talk of the RLC filter. Both signals have been shifted to 0° for comparison purposes.

3.7 Mixers

The following discussion of mixers was adapted from the Mini-Circuits RF designers handbook [44].

A mixer is a circuit which accepts to a radio frequency (RF) signal and a local oscillator (LO) and then multiplies them to form the sum and difference frequencies (intermediate frequencies (IF)).

$$\cos(\omega_{RF}t)\cos(\omega_{LO}t) = \frac{1}{2}\cos(\omega_{RF}t + \omega_{LO}t) + \frac{1}{2}\cos(\omega_{RF}t - \omega_{LO}t) \tag{3.17}$$

Although any non-linear component will mix two frequencies (for example a diode, as shown in figure 3.18a), a double-balanced mixer as shown in figure 3.18b, will reduce the amount leakage between the RF, IF and LO signals.

The symmetry of the double-balanced mixer's configuration provides the isolation between the RF and LO and IF ports. Although the full description of how the isolation is achieved is beyond the scope of this discussion, we will review the concepts by examining a simpler circuit. Figure 3.18c is a single balanced mixer. A single-balanced mixer offers good isolation between the LO and RF ports, but does not isolate the RF and the IF ports. Figure 3.18d is an equivalent description of the circuit. If the two diodes are equivalent, then the currents drawn, i_{lo1} and i_{lo2} will be equal in amplitude and phase. Therefore at the IF port, the LO signal will exactly cancel, isolating the LO from the IF.

The mixers we use were purchased from MiniCircuits (ZFM-4). Our mixers have a RF frequency range from 5 - 1250 MHz and an intermediate frequency range from DC to 1250 MHz.

3.8 Summary

The phase modulation device which we used evolved over the years. The components that changed during the experiments in this work were the signal generators and the band-pass filters. Although we tested various photon detectors, all of the experiments performed here used a photomultiplier tube.

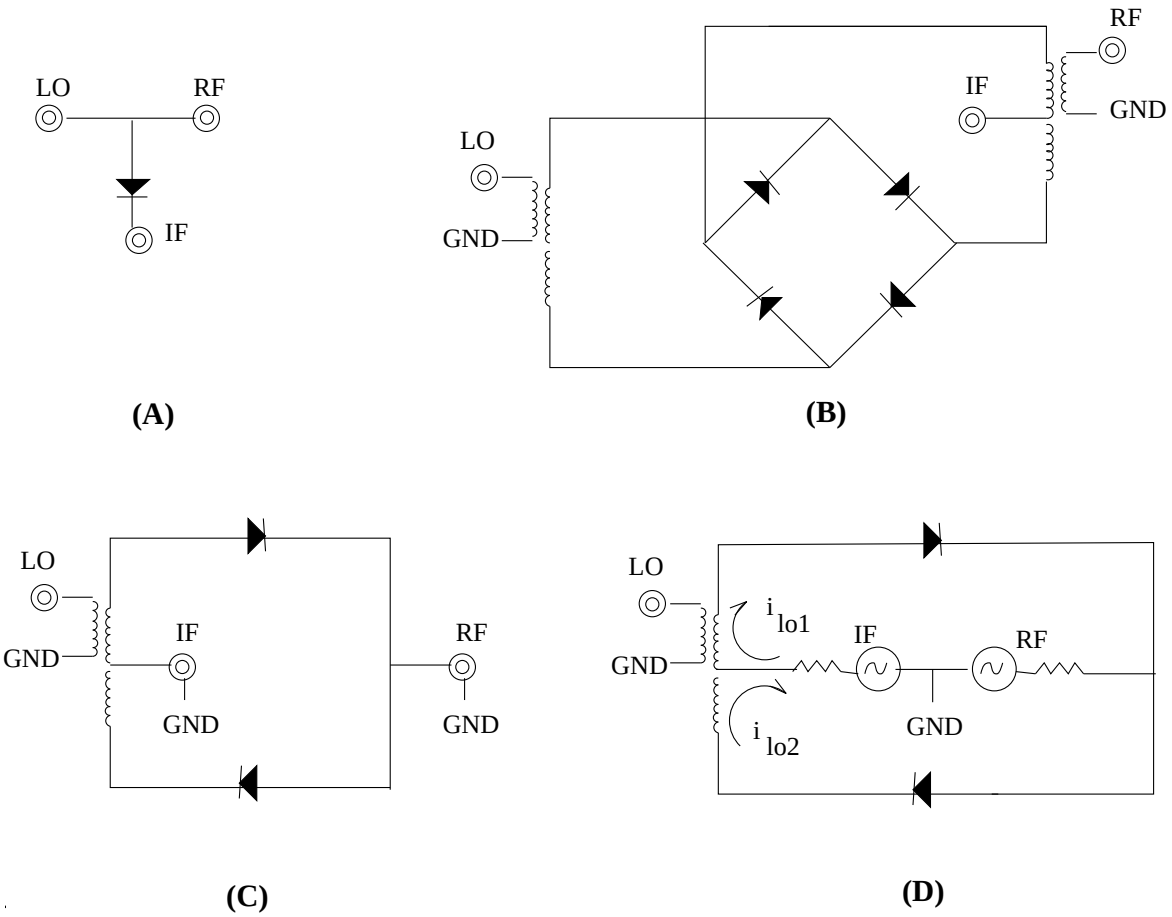

Figure 3.18: (a) A simple mixer (b) A double balanced mixer designed to isolate the local oscillator (LO), the radio frequency oscillator (RF) and the intermediate frequency (IF). (c) A single balance mixer provides isolation between the LO and RF ports. (d) An equivalent circuit for the single balanced mixer.

The initial experiments demonstrating the existence and properties of DPDW (presented in chapter 2) used a system composed of the twin-T band-pass filter and the home-made radio oscillators. Most of the absorption and scattering images were created using the radio transceivers and the twin-T band-pass filters. The absorption calibration curve was created using the radio transceivers and the LC band-pass filters.